

Phase Transitions in Swollen Networks. 3. Swelling Behavior of Radiation Cross-Linked Poly(vinyl methyl ether) in Water[†]

R. Moerkerke, F. Meeussen, R. Koningsveld, and H. Berghmans*

Laboratory for Polymer Research, Katholieke Universiteit Leuven, Celestijnenlaan 200F, B-3001 Heverlee, Belgium

W. Mondelaers

Institute of Nuclear Science, Rijksuniversiteit Gent, Proeftuinstraat 68, B 9000 Gent, Belgium

E. Schacht

Polymer Materials Research Group, Department of Organic Chemistry, University of Gent, Krijgslaan 281, S4-bis, B-9000 Gent, Belgium

K. Dušek

Institute of Macromolecular Chemistry, Academy of Sciences of the Czech Republic, 162 06 Prague 6, Czech Republic

K. Šolc

Central Michigan University, Department of Physics, Mt. Pleasant, Michigan 48859

Received October 15, 1997; Revised Manuscript Received January 22, 1998

ABSTRACT: It is demonstrated that the collapse of gels of radiation cross-linked poly(vinyl methyl ether) swollen in water is a truly discontinuous process obeying classic thermodynamic principles. The phenomenon can further be shown to be related to the relevant type of limiting critical demixing of solutions of the corresponding non-cross-linked polymer. There are three such types, including "classic" Θ behavior, and they can also be recognized in the swelling behavior of the cross-linked analogue.

Introduction

In the last few decades responsive gels have been the subject of extensive research,^{1,2} motivated by a wide range of potential applications. The latter include widely varying fields such as biomedical applications, as for example, drug delivery systems and enzyme activity controlling devices,^{3,4} and chemomechanical systems.⁵ Chemically cross-linked poly(*N*-isopropylacrylamide) (NIPA), made by copolymerization, and radiation cross-linked poly(vinyl methyl ether) (PVME) hydrogels have frequently been used as model systems in the investigation of responsive swelling behavior.^{1,2}

The phase relationships associated with responsive behavior can be described by the usual Gibbs-free-energy function, including a polymer–solvent interaction parameter that depends markedly on the polymer concentration. This was indicated by Dušek and Prins⁶ and worked out in detail in part 1 of this series.⁷ Part 2 dealt with swelling equilibria in binary solvents.⁸

The introduction of a concentration-dependent interaction parameter has since long been known to supply an effective tool to bring theoretical predictions and experimental reality closer together. Staverman showed in 1937 that disparity in size and shape between the component molecules of a mixture provides an important reason for the interaction parameter to depend on concentration.⁹ Later, application to polymer systems

has been suggested by a number of authors, i.e. Tompa.¹⁰ In a recent paper we demonstrated that the system water/PVME represents a particularly striking case in point.¹¹ It is the objective of the present paper to extend these considerations to cross-linked PVME, swollen in water.

Model

Non-Cross-Linked Systems. When solutions of linear polymers with very high molar mass show partial miscibility, the liquid–liquid critical state usually occurs at very small polymer concentration. The latter tends to zero if the molar mass goes to infinity (Θ state).¹² Indications of possible complications with respect to this generally accepted rule have been reported occasionally,^{13–16} and their origin could be related to a strong dependence of the interaction parameter on concentration. This feature has been the subject of a recent phenomenological analysis in which three types of limiting critical behavior could be distinguished.¹⁷ The above-mentioned "classic" Θ behavior (type I) is characterized by a limiting critical concentration for infinite molar mass, ϕ_{2L} , equal to zero. With type II, a single off-zero limiting critical concentration, ϕ_{2L} , occurs at non- Θ conditions. With type III there are two off-zero limiting critical concentrations, in addition to the usual zero critical concentration. The three types of phase behavior, mentioned above, are schematically illustrated in Figure 1a–c that were calculated with the expression for ΔG , the Gibbs energy of mixing, developed by Flory,^{12,18,19} Huggins,^{20,21} and Staverman and

[†] Respectfully dedicated to the memory of professor J. J. Hermans, deceased January 10, 1997.

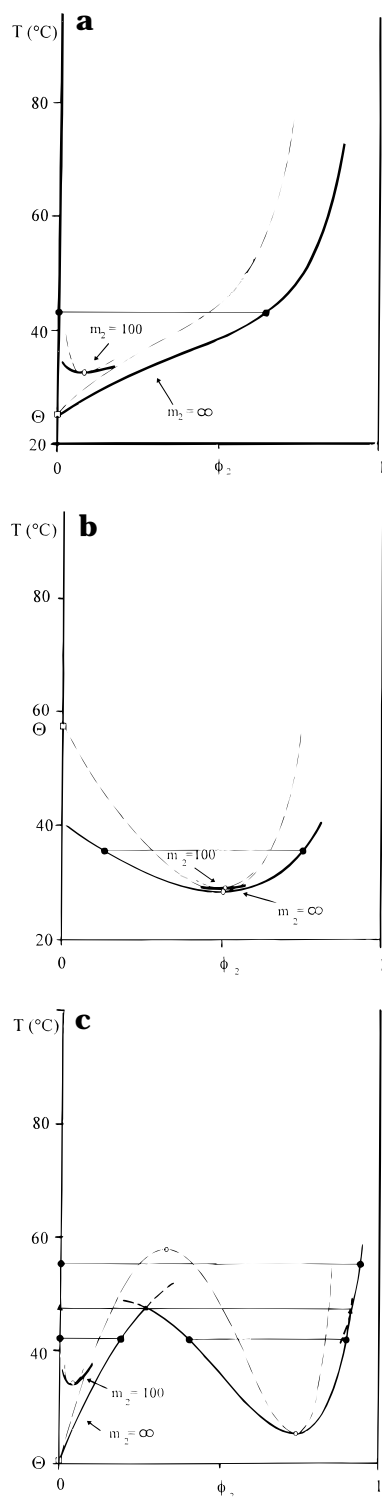


Figure 1. Demixing patterns in binary polymer solutions, from ref 11: (a) type I ($g_1 = 0.1$, $g_2 = 0.3$); (b) type II ($g_1 = 2/3$, $g_2 = 0$); (c) type III ($g_1 = -0.0125$, $g_2 = 1.25$); (○) critical point; (□) limiting critical point; (dashed line) spinodal; (heavy curve) binodal; (●—●) tie line; Θ, theta point; (▲—▲—▲) three-phase line. In all figures, $g_{0h} = -1700$ K and $g_{0s} = 6.3$.

Van Santen,^{22,23}

$$\Delta G/NRT = (\phi_1/m_1) \ln \phi_1 + \sum (\phi_{2i}/m_{2i}) \ln \phi_{2i} + \phi_1 \phi_2 g(T, \phi_2) \quad (1)$$

where ϕ_1 and ϕ_{2i} are the volume fractions of solvent and species i in the polymer, respectively; $\phi_2 = \sum \phi_{2i}$. The

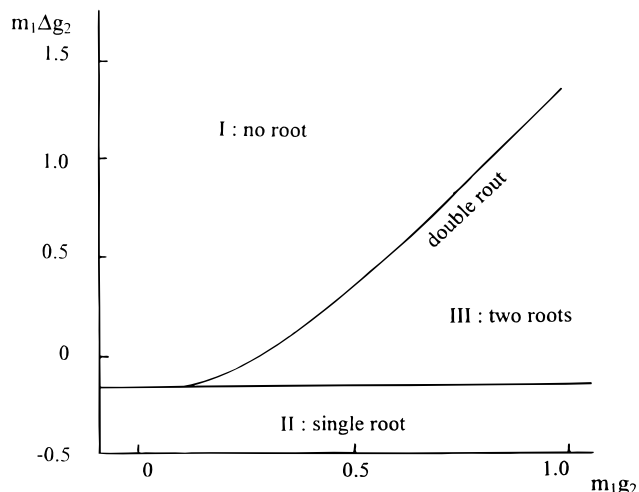


Figure 2. Regions in interaction-coefficient space of types I–III limiting critical behavior, from ref 11.

total volume is built up of N moles of identical basic volume units (BVUs), and m_1 and m_{2i} represent the number of BVUs occupied by a single solvent molecule and a macromolecule i , respectively. The interaction function g is here represented by a truncated polynomial,

$$g = g_0 + g_1 \phi_2 + g_2 \phi_2^2 \quad (2)$$

the coefficients may depend on temperature T , for instance by $g_i = g_{is} + g_{ih}/T$. It is seen in Figure 1 that the values of g_1 and g_2 determine the type of phase behavior, which can be summarized in a mapping of $\Delta g_2 (=g_2 - g_1)$ against g_2 (Figure 2).¹¹

Cross-Linked Systems. Equations 1 and 2 can be used to describe the swelling behavior of a network in a single solvent.⁷ The expression for the Gibbs energy now has two contributions, one for the mixing of network and the solvent and one due to the elasticity of the network. This results in

$$\Delta G/NRT = (\phi_1/m_1) \ln \phi_1 + G_{ab} + \phi_1 \phi_2 g(T, \phi_2) \quad (3)$$

G_{ab} , the elastic contribution to ΔG , is defined by

$$G_{ab} = \Delta G_{el}/NRT = (3A/2m_c)\Phi_0^{2/3}(\phi_2^{1/3} - \phi_2) + (B/m_c)\phi_2 \ln \phi_2 \quad (4)$$

where Φ_0 is the polymer volume fraction at network formation, A and B are the well-known front factors (see ref 7), and m_c is the average number of BVUs in the polymer chains between two cross-links in the network. The interaction function g is defined by eq 2.

We now check whether the values of g_1 and g_2 , determining the type of limiting phase behavior for non-cross-linked systems, have a similar influence on the swelling behavior of cross-linked systems. Parts a–c of Figures 3 show the calculated phase diagrams of cross-linked systems, for the g_1 and g_2 values used for Figure 1a–c. It is seen that type I limiting behavior (“classic” Θ behavior) is associated with a continuous swelling curve (Figure 3a). Both type II and type III apparently go with discontinuous swelling behavior (Figure 3b,c), as discussed in ref 7.

It is useful to consider the two important general consequences of cross-linking: (a) the molar mass of the

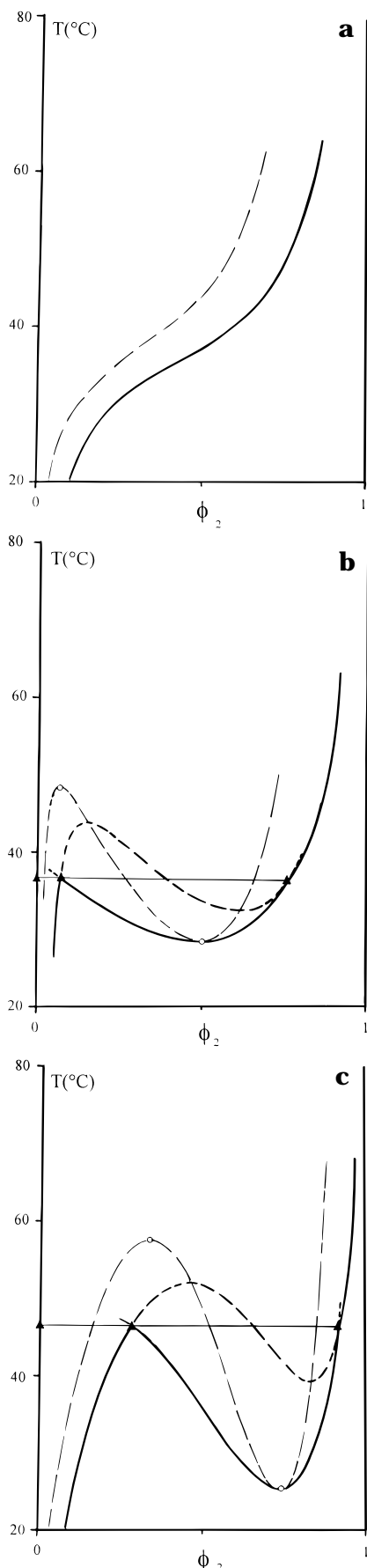


Figure 3. Phase diagrams of cross-linked systems calculated with eq 3. The parameter values of g are the same as used for Figure 1, $m_c = 100$, $f = 3$ (f = functionality of the network). Symbols are as in Figure 1.

polymer becomes infinite; (b) the system cannot reach a state of infinite dilution.

Cross-linking of a system exhibiting type I limiting critical behavior makes the molar mass infinite, and for that reason the critical point would tend to go to the $\phi_{2L} = 0$ limit, but this state cannot be reached due to the impossibility of infinite dilution. The maximum degree of dilution is determined by the degree of cross-linking and depends on T , as is indicated by the swelling curve in the phase diagram. Such systems therefore show a continuous transition from the highly swollen state to a smaller degree of swelling.

A linear polymer solution exhibiting type II limiting critical behavior will, at infinite molar mass, separate into two liquid phases, one of a higher and the other of a lower concentration. The latter phase concentration approaches zero when the temperature is raised (Figure 1b). The latter phenomenon is impossible if the molar mass becomes infinite due to cross-linking, and there must occur a swelling curve for the pure solvent/swollen network equilibrium. The swelling curve will interfere with the miscibility gap, and this interference causes a three-phase equilibrium between a pure solvent phase and two swollen phases, one of which is highly swollen whereas the other one is contracted. A three-phase equilibrium is nonvariant in a binary system at a fixed pressure, hence the discontinuity in the swelling behavior.

Linear type III systems are already characterized by a discontinuity due to three-liquid-phase equilibrium. Cross-linking now prevents the left-hand miscibility gap of Figure 3c from terminating in the Θ point at $\phi_2 = 0$ (at about 20 °C) and forces the solvent/swollen network equilibrium curve to follow the usual swelling-curve behavior below the three-phase temperature.

It is important to note that the occurrence of discontinuous swelling behavior is not only determined by the parameter values g_1 and g_2 , but also by the cross-link density. When the latter is too high (m_c too small), there is no miscibility gap and the swelling curve shifts toward the polymer-rich side of the diagram. The values of m_c used for Figure 3 were chosen properly.⁶

Experimental Section

1. Materials. PVME was purchased from Aldrich.

The molar-mass distribution and its averages were determined by GPC in THF as the solvent. This determination resulted in a weight average of $M_w = 60.5$ kg/mol and a number average of $M_n = 20.5$ kg/mol, leading to a polydispersity of $M_w/M_n = 3$.

2. Cross-Linking of PVME. Experimental Procedure.

Two types of ionizing radiation are useful for radiation-induced cross-linking: photons and electrons. The irradiation devices can be divided in two groups: radioisotopes and electron accelerators. The classical radioisotopes emit γ rays (e.g., the ^{60}Co photon energies are 1.173 and 1.333 MeV). The beams of electron accelerators can be applied in two ways. The charged beam emerging from the accelerator can be used directly for treatment of the samples. Very high radiation dose rates can be obtained in this way, but it is very difficult to control the temperature of the irradiated samples. Alternatively, the electron beam can be converted into X-rays (also called bremsstrahlung) by being made to strike a conversion target: the electrons are decelerated in a high-atomic-number absorber, and a part of their kinetic energy emerges in the form of bremsstrahlung X-rays. The lower dose rates of X-ray beams allow the application of a thermostatic circuit to keep the sample at a constant temperature.

Preparation of the Gels. Solutions of 10 wt % PVME in deionized water are enclosed in a cylindrical sample cell with

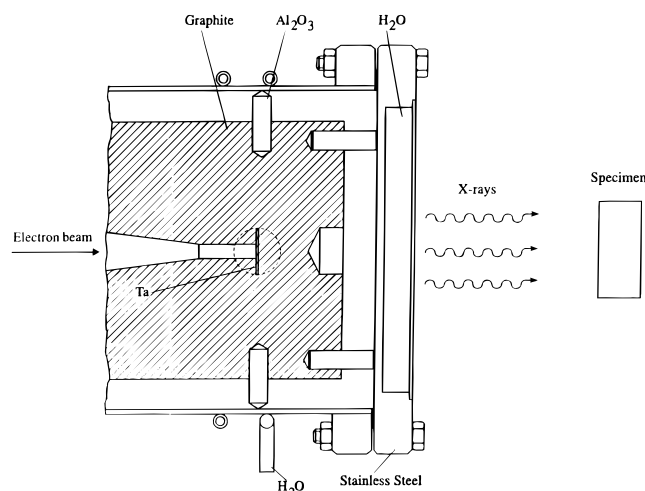


Figure 4. Bremsstrahlung production configuration.

a flat bottom so that free space was available above the solution. This prevents the sample from being put under any form of constraint during the irradiation procedure. The solutions are degassed before their introduction in the sample holder, which is then sealed under an argon atmosphere. The samples are irradiated at 16 °C with different doses of 60 and 80 kGy. The samples are put into an experimental setup that guarantees a constant temperature inside the sample during the whole irradiation process. Such an accurate temperature control prevents any phase separation taking place during the irradiation.¹¹

The samples are irradiated with X-rays from the 15 MeV linear electron accelerator of the Department of Subatomic and Radiation Physics, University of Gent.²⁴ This accelerator can deliver electron beams with a well-defined energy in the range between 3 and 15 MeV and with an average power up to 20 kW. Because of the high electron beam powers hitting the Bremsstrahlung converter, a tantalum foil embedded in radiation-cooled graphite is used, as shown in Figure 4. For this experiment, the X-ray beam is produced with 500 μ A of 10 MeV electrons. The photons emitted from the bremsstrahlung configuration have spread in energy from several 10 keV up to the energy of the electrons, the average energy being 1.6 MeV. The dose rates are 80 kGy/h.

Prior to the irradiation, the homogeneity of the dose delivered to the specimen is verified with an ionization chamber on a motor-driven scanning system. Absolute dose calibration is performed with a chemical dosimeter using a ferrous sulfate Fricke solution. This dosimeter uses the change in ultraviolet absorption caused by dose-dependent oxidation of ferrous to ferric ions.

After irradiation, the gels are removed from the sample container and non-cross-linked polymer is extracted with acetone in a Soxhlet apparatus for 2 weeks. After the extraction, the samples are dried under vacuum.

Determination of the Degree of Swelling. The degree of swelling of the gels is determined by weighing. At regular times the gel is taken out of the water, surface-dried, and weighed on an analytical balance.

Calorimetry. A Setaram DSC111-Micro calorimeter is used. Calibration is performed with indium ($T_m = 156.6$ °C) and sodium sulfate decahydrate ($T_{dh} = 32.38$ °C) (first dehydration temperature). Scanning rates of 0.1 and 1 °C/min have been used with samples of about 50 mg. The samples are prepared by adding the appropriate amount of water to a well-known amount of dry polymer network in the sample container and the sample container is then sealed.

Results

1. Swelling Curves. The temperature dependence of the degree of swelling of the different samples has been investigated. The swelling data are presented as

the weight fraction of PVME network in the gel as a function of the temperature. A weight fraction of 0.1 means that the final weight of the gel at swelling equilibrium equals 10 times the weight of the dry network. The equilibrium degree of swelling at room temperature, a measure of the degree of cross-linking, is obtained by immersing the samples in an excess of water at room temperature until no further uptake of water is detected. The temperature dependence of this equilibrium degree of swelling is determined in two different ways. The first consists of a stepwise heating of the sample, swollen to equilibrium at room temperature. After every increase of 1 °C, the sample is kept at the new temperature until the equilibrium degree of swelling is reached. The second procedure consists of swelling the dry network to equilibrium in an excess amount of water at constant temperature.

Parts a and b of Figure 5 represent the swelling curves of the different networks. The equilibrium degree of swelling obtained by swelling at room temperature is inversely proportional to the irradiation dose. Therefore we may conclude that an increase in the irradiation dose results in an increase of the degree of cross-linking. From room temperature to 35.5 °C, the experimental points were obtained by stepwise heating of samples swollen to equilibrium at room temperature. At the high concentration side, equilibrium swelling was obtained by starting from the completely dry network. Some of the experimental points were obtained at the same temperature by the two different methods. They lead to the same equilibrium degree of swelling. The equilibrium character of the experimental points was further supported by the swelling at room temperature of a sample, initially swollen at 38 °C (low degree of swelling).

At high and low solvent content, the change of the degree of swelling with temperature is limited. A discontinuity in the swelling curve is observed at 36 °C.

2. Gel–Gel Demixing. The calculated phase diagram represented in Figure 3c suggests the presence of a gel–gel (g–g) demixing domain, which interferes with the swelling curve, resulting in an invariant three-phase equilibrium. Such a g–g demixing can be studied by different techniques. One of them is calorimetry, and this possibility has been discussed in the literature.^{25,26} The technique has been applied with success to different polymer solvent systems^{27–35} and more particularly to the system linear PVME/water.¹¹ The obtained experimental data revealed the occurrence of type III demixing behavior. The relative high enthalpy changes involved in the system linear PVME/water make it possible to observe L–L (liquid–liquid) demixing by this technique even at low polymer weight fractions. The technique was therefore applied in the study of the g–g demixing in the cross-linked systems. Networks prepared with an irradiation dose of 60 kGy were investigated. Data were collected at two different scanning rates.

Typical thermograms are presented in Figure 6a,b. The demixing is endothermic, and the behavior is similar to that of the linear material.^{11,34,36} The peak obtained with $w_2 = 0.60$ is clearly composed of two parts: a broad onset, followed by a sharp peak. Such a demixing signal is characteristic for the occurrence of two consecutive demixing processes: one that is smeared out over a broad temperature range and another that proceeds in a very narrow temperature range. Two demixing temperatures can be deduced: the tempera-

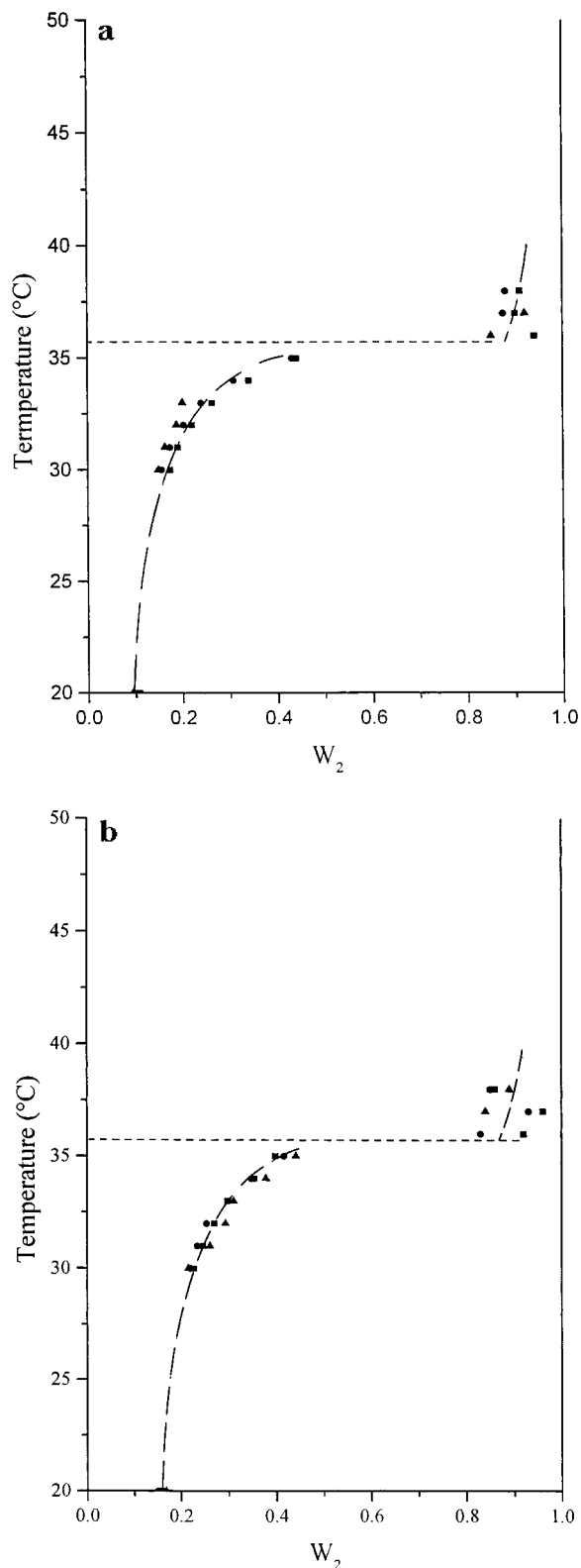


Figure 5. Swelling curves of cross-linked PVME in water: (a) dose 60 kGy; (b) dose 80 kGy. Three different symbols: data of three samples. (Curves were hand drawn to guide the eye.)

ture at the beginning of the broad first part of the signal (T_b) and the temperature at the onset of the sharp signal (T_o). These two temperatures are indicated in Figure 6a. At lower polymer content ($w_2 = 0.05$) the sharp peak is clearly visible and T_o can clearly be localized. The localization of T_b on the contrary is more difficult as the signal seems to be smeared out over a large temperature

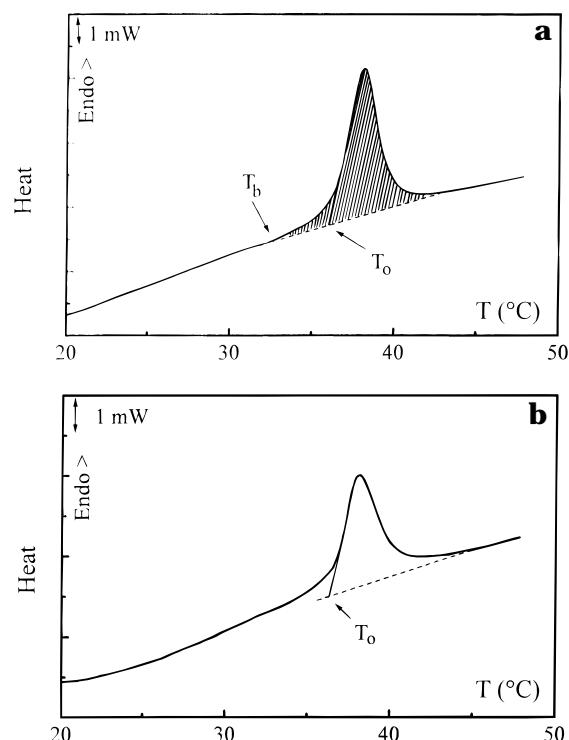


Figure 6. DSC thermogram obtained by heating a sample of cross-linked PVME (60 kGy) swollen in water using a Setaram DSC 111, scanning rate 1 °C/min: (a) $w_2 = 0.60$; (b) $w_2 = 0.05$.

domain. The analysis was therefore limited to T_o . The values of the two transitions temperatures are plotted as a function of the concentration in Figure 7a,b. The onset temperature of the sharp peak, T_o , shows little concentration dependence in the concentration range investigated. The most accurate data are obtained at the lowest scanning rate, which gives the best resolution of the endothermic signals. This transition temperature can therefore be considered as invariant. The concentration dependence of T_b is more complex, and the most reliable data are obtained at a scanning rate of 1 °C/min (Figure 6a). At this scanning rate, the broad endothermic signal can be observed with enough accuracy. At a scanning rate of 0.1 °C/min, this signal almost disappears in the baseline and any attempt to localize T_b leads to too high, not very reliable values (Figure 6b). At $w_2 \leq 0.40$, the endothermic signal corresponds to the deswelling of the network. At $w_2 > 0.42$, T_b goes through a minimum and delimits the LCST miscibility gap. The demixing temperatures, although obtained by dynamic observations, coincide very well with those obtained from equilibrium swelling experiments. No influence of the scanning rate could be investigated as the exact localization of the "beginning temperature" (T_b) becomes more difficult as the scanning rate is lowered.

3. Heat of Transition. Integration of the shaded area in Figure 6a yields the enthalpy of transition for the considered concentration. These enthalpy values are plotted as a function of the polymer content in Figure 8, together with the data obtained with the linear system. There is a good agreement between the two sets of data¹¹ in the low and the high polymer content region. In the intermediate region, the values of the non-cross-linked system are higher. This deviation between the two sets of data is the subject of current research.

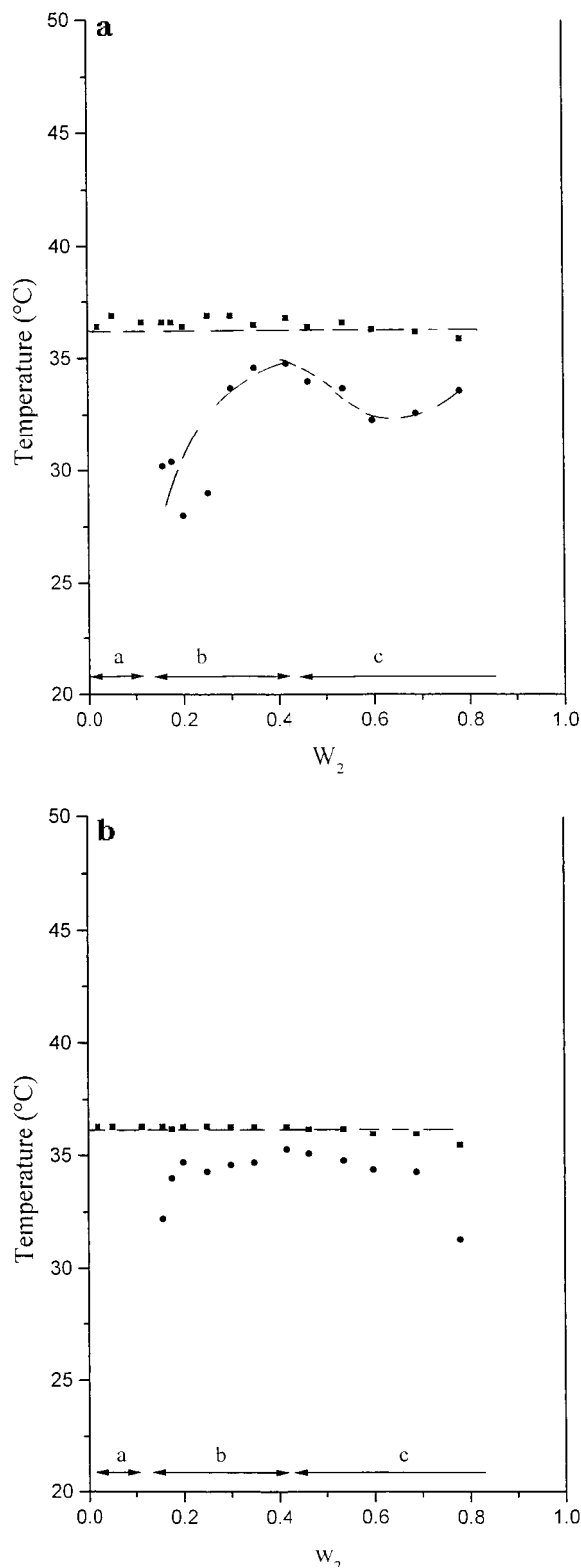


Figure 7. Phase diagrams derived from DSC measurements (curves hand drawn to guide the eye) of the 60 kGy PVME network: (■) onset temperature T_0 ; (●) demixing temperature T_b ; (a) scanning rate 1 °C/min; (b) scanning rate 0.1 °C/min.

Discussion

The present results establish that the cross-linked PVME system exhibits a discontinuous swelling behavior in water. These samples also show the LCST type demixing behavior in the high polymer concentration domain, as predicted for a non-cross-linked system with

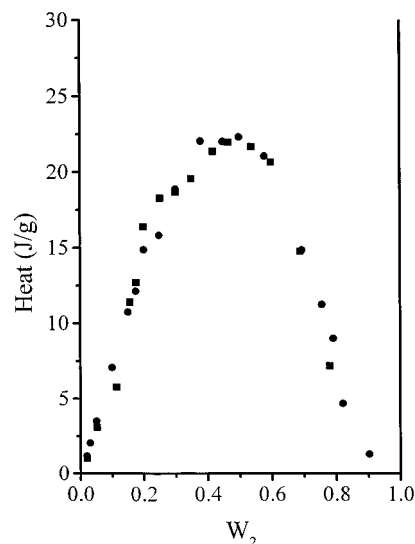


Figure 8. Heat of transition of linear PVME (from ref 11) (●) and cross-linked PVME (60 kGy) in water from DSC measurements (■).

type III demixing behavior. The results of the calorimetric observations of the demixing are in very good agreement with the proposed demixing model.

At higher polymer content (c region in Figure 7a,b) the two consecutive demixing processes can clearly be identified.

In the intermediate concentration region (b), the endothermic signal corresponds to the deswelling of the network with increasing temperature. The demixing temperature can be localized with good accuracy, and the onset of this signal is clearly defined. At low temperature, the solvent content of the network is lower than the one that corresponds to the equilibrium degree of swelling at that temperature. On heating, the equilibrium swelling curve will be reached so that further heating leads to a deswelling of the network. The pronounced curvature of the deswelling curve prevents the demixing signal from being smeared out over a too broad temperature domain.

Demixing observed in the low concentration region (a) corresponds also to the deswelling of the network. But the correct observation of T_b is almost impossible for two reasons. At this polymer content, the swollen network is in equilibrium with pure water and at any temperature the network has already reached its equilibrium degree of swelling. An increase in temperature will bring the sample into the two-phase region, and the demixing endotherm sets in as soon as the temperature is raised. This makes the observation of the onset of this process with a dynamic calorimeter impossible. The heat exchange is very small and is smeared out over a very broad temperature domain: at low temperature, the equilibrium swelling curve is almost vertical.

The concentration-insensitive onset temperature of the sharp endothermic signal clearly supports the existence of an invariant, three-phase equilibrium. The combination of such a demixing behavior with the invariant swelling behavior clearly demonstrates that the system cross-linked PVME/water follows the model represented in Figure 3c.

Acknowledgment. The authors thank the Flemish Institute for the Promotion of Scientific-Technological Research in Industry (IWT) for a fellowship for R.M and

F.M. They also thank the National Fund for Scientific Research and the Interuniversity Poles of Attraction, Belgian State, Prime Ministers Office for Scientific, Technical, and Cultural Affairs (IUAP III/16 and IV-P4/11) for financial support. This work was in part supported by a Concerted Research Project of the University of Ghent (GOA 12050695). K. Š. thanks the U.S.-Czech Science and Technology Program, Project Number 95024, for partial support.

References and Notes

- (1) *Advances in Polymer Science*, Springer: Berlin, 1993; Vols. 109–110.
- (2) *Polymer Gels and Networks*; Elsevier: New York, 1993, Vols. 4–6.
- (3) Okano, T.; Bae, Y. H.; Jacobs, H.; Kim, S. W. *J. Controlled Release* **1990**, *11*, 255.
- (4) Park, T. G.; Hoffman, A. S. *Appl. Biochem. Biotechnol.* **1988**, *19*, 1.
- (5) Suzuki, M.; Ushida, T.; Fujishige, S.; Takeishi, T. *Biorheology* **1986**, *23*, 274.
- (6) Dušek, K.; Prins, W. *Adv. Polym. Sci.* **1969**, *6*, 1.
- (7) Moerkerke, R.; Koningsveld, R.; Berghmans, H.; Dušek, K.; Šolc, K.; *Macromolecules* **1995**, *28*, 1103.
- (8) Moerkerke, R.; Koningsveld, R.; Berghmans, H.; Dušek, K.; Šolc, K. *Wiley Networks Group Rev.* **1998**, *1*, 463.
- (9) Staverman, A. J. *Recl. Trav. Chim.* **1937**, *56*, 885.
- (10) Tompa, H. *Compt. Rend. Soc. Chim. Phys., Paris* **1952**, 163.
- (11) Schäfer-Soenen, H.; Moerkerke, R.; Koningsveld, R.; Berghmans, H.; Dušek, K.; Šolc, K.; *Macromolecules* **1997**, *30*, 410.
- (12) Flory, P. J. *Principles of Polymer Chemistry*; Cornell University Press: 1953, Chapter XIII.
- (13) Flory, P. J.; Daoust, H. *J. Polym. Sci.* **1957**, *25*, 429.
- (14) Dušek, K. *Collect. Czech. Chem. Commun.* **1969**, *34*, 3309.
- (15) Koningsveld, R.; Kleintjens, L. A. *Pure Appl. Chem., Macromol. Chem.* **1973**, *8*, 197.
- (16) Nies, E.; Koningsveld, R.; Kleintjens, L. A. *Prog. Colloid Polym. Sci.* **1985**, *71*, 2.
- (17) Šolc, K.; Dušek, K.; Koningsveld, R.; Berghmans, H. *Collect. Czech. Chem. Commun.* **1995**, *60*, 1661.
- (18) Flory, P. J. *J. Chem. Phys.* **1941**, *9*, 660.
- (19) Flory, P. J. *J. Chem. Phys.* **1942**, *10*, 51.
- (20) Huggins, M. L. *J. Chem. Phys.* **1941**, *9*, 440.
- (21) Huggins, M. L. *Ann. N. Y. Acad. Sci.* **1942**, *43*, 1.
- (22) Staverman, A. J.; Van Santen, J. H. *Recl. Trav. Chim. Pays-Bas* **1941**, *60*, 76.
- (23) Staverman, A. J. *Recl. Trav. Chim. Pays-Bas* **1941**, *60*, 640.
- (24) Mondelaers, W.; Van Laere, K.; Goedefroot, A.; Van den Bossche, K. *Nucl. Instrum. Methods* **1996**, *A368*, 278.
- (25) Maderek, E.; Wolf, B. A. *Polym. Bull.* **1983**, *10*, 458.
- (26) Arnauts, J.; De Cooman, R.; Vandeweerdt, P.; Koningsveld, R.; Berghmans, H. *Thermochim. Acta* **1994**, *238*, 1.
- (27) Arnauts, J.; Berghmans, H. *Polym. Commun.* **1987**, *28*, 66.
- (28) Arnauts, J.; Berghmans, H. In *Physical networks, polymers and gels*; Burchard, W., Ross Murphy, S. B., Eds.; Elsevier: New York, **1990**, p 33.
- (29) Arnauts, J.; Berghmans, H.; Koningsveld, R. *Makromol. Chem.* **1993**, *194*, 77.
- (30) Vandeweerdt, P.; Berghmans, H.; Tervoort, Y. *Macromolecules* **1991**, *24*, 3457.
- (31) Berghmans, H.; Deberdt, F. *Philos. Trans. R. Soc. London A* **1994**, *348*, 117.
- (32) Callister, S.; Keller, R.; Hikmet, R. M. *Makromol. Chem., Macromol. Symp.* **1990**, *39*, 19.
- (33) Vandeweerdt, P.; Decooman, R.; Berghmans, H.; Meijer, H. *Polymer* **1994**, *35*, 5141.
- (34) Maeda, H. *J. Polym. Sci., Polym. Phys. Ed.* **1994**, *32*, 91.
- (35) Soenen, H.; Berghmans, H. *J. Polym. Sci., Polym. Phys. Ed.* **1996**, *34*, 241.
- (36) Buthenuth, M.; Jenckel, E. *Naturwissenschaften* **1956**, *43*, 276.

MA971512+